Catalysis Communications 14 (2011) 114–117

Contents lists available at ScienceDirect

Catalysis Communications

journal homepage: www.elsevier.com/locate/catcom

Short Communication

The synthesis and investigation of ruthenium phosphide catalysts

Qingxin Guan, Cuiping Sun, Rongguan Li, Wei Li *

Key Laboratory of Advanced Energy Materials Chemistry (Ministry of Education), College of Chemistry, Nankai University, Tianjin, 300071, China

ARTICLE INFO

Article history:
Received 7 July 2011
Received in revised form 1 August 2011
Accepted 1 August 2011
Available online 7 August 2011

Keywords:
Hydrodesulfurization
Hydrodenitrogenation
Hypophosphite
Thermal decomposition
Ruthenium phosphide

ABSTRACT

Highly active Ru_2P/MCM-41 and RuP/MCM-41 catalysts were synthesized by thermal decomposition of ruthenium chloride and hypophosphite precursors. The effect of experimental conditions on the final products is discussed. The results of investigation show that the reaction mechanism of ruthenium phosphide is different from nickel phosphide. Catalytic properties were tested for the hydrodesulfurization of dibenzothiophene and hydrodenitrogenation of quinoline. The results showed that both Ru_2P/MCM-41 and RuP/MCM-41 catalysts exhibited higher activities than Ru/MCM-41.

1. Introduction

Metal phosphides have attracted considerable attention for their wide applications in many fields; for instance, superconductivity, magnetocaloric behavior, catalytic activity, and lithium intercalation capacity etc.[1–5]. As a kind of hydroprocessing catalysts, supported transition metal phosphides have recently been reported to be promising for its high-performance and high-stability compared to transition metal carbides and nitrides [6–9]. Recent studies have shown that the noble metal phosphide catalysts, except Pt, showed higher HDS activities than noble metal catalysts [10]. In our previous published papers [11,12], Ni_2P, Cu_3P, MoP and InP were synthesized using the decomposition of hypophosphites, which is a simple and safe method. However, the synthesis of noble metal phosphides using the decomposition of hypophosphites method has not been reported. Herein, we tried to synthesize highly active ruthenium phosphide catalysts to achieve the HDS and HDN for gasoline and diesel oil.

The structure model of Ru, Ru_2P, and RuP is given in Fig. 1, which was built from the data of Inorganic Crystal Structure Database (ICSD) [13–15]. Only a few methods were available to synthesize ruthenium phosphide, including RuP was synthesized by the direct reduction of phosphate in hydrogen [5], RuP was synthesized in a silica xerogel matrix from single-source molecular precursors [16], Ru_2P catalysts were prepared by temperature-programmed reduction (TPR) method [10]. Different from the above methods, this paper mainly focus on the synthesis of Ru_2P and RuP from the thermal decomposition of ruthenium chloride and hypophosphite mixed precursors. Similar to our previous research [11,12], mesoporous siliceous MCM-41 zeolite was used as carrier to synthesize supported ruthenium phosphide catalysts. The catalytic properties of different catalysts were evaluated by HDS of dibenzothiophene (DBT) and HDN of quinoline. For comparison, the Ru/MCM-41 and commercial NiMoWS/Al_2O_3 catalysts were also tested under the same conditions.

2. Experimental

2.1. Catalyst preparation

Ruthenium phosphide was prepared by the thermal decomposition of ruthenium chloride and hypophosphite mixed precursors. In a molar ratio ($NaH_2PO_2/RuCl_3$) of 3.5, $RuCl_3{\cdot}3H_2O$ and $NaH_2PO_2{\cdot}H_2O$ were dissolved in deionized water under stirring at room temperature. Subsequently, a red solid precursor was obtained after the solution was evaporated slowly to dehydrate and dried at 333 K for 12 h. Then, the precursor was heated at the required temperature for 0.5 h in a static Ar atmosphere. Finally, the product was cooled to ambient temperature under flowing Ar, washed three times with deionized water, and dried at 120 °C for 3 h. To prepare the supported ruthenium phosphide by incipient wetness method, a certain amount of support was impregnated with the solution described above. The precursor was dried at 333 K for 12 h, and the remaining steps were similar to those described above.

2.2. Catalyst characterization

Powder X-ray diffraction (XRD) patterns were collected using a Bruker D8 Focus diffractometer, with Cu Kα at 40 kV and 40 mA between 3° and 80° (2θ) with a step length of 1 s. Nitrogen adsorption–

* Corresponding author. Tel./fax: +86 22 23508662.
E-mail address: weili@nankai.edu.cn (W. Li).

1566-7367/$ – see front matter © 2011 Elsevier B.V. All rights reserved.
doi:10.1016/j.catcom.2011.08.005

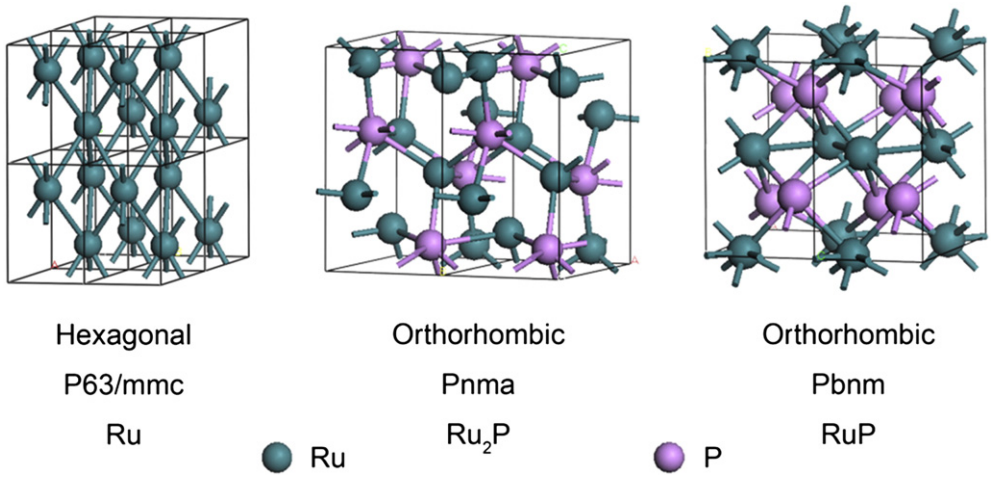

Fig. 1. The structure model of Ru, Ru_2P, and RuP.

desorption isotherms of samples at 77 K were measured using a BEL-MINI adsorption analyzer. Samples were degassed at 473 K for 3 h before measurement. The surface area was calculated using a multi-point Brunauer–Emmett–Teller (BET) model. The pore size distribution was obtained from the desorption isotherms using the Barret–Joyner–Halenda (BJH) model, and the total pore volume was estimated at a relative pressure of 0.99, assuming full surface saturation with nitrogen. H_2-TPR and CO chemisorptions of the catalysts were performed using Micromeritics ChemSorb 2750 gas adsorption equipment. The sample was loaded into a quartz reactor and pretreated in 10% H_2/Ar at 450 °C for 3 h. After cooling in He, pulses of 10% CO/He in a He carrier (25 cm^3 (NTP) min^{-1}) were injected at 30 °C through a loop tube.

2.3. Catalyst test

The HDS and HDN catalytic activities were evaluated using 3000 ppm dibenzothiophene (DBT) and 3000 ppm quinoline in decalin. The HDS and HDN reactions were carried out in a continuous-flow fixed-bed microreactor. The catalyst was crushed and sieved to the 20–40 mesh size range. 1.00 g of catalyst was diluted with SiO_2 to a volume of 5.0 mL in the reactor. Prior to reaction, catalysts were pretreated in situ with flowing H_2 (50 mL min^{-1}) for 2 h. The test conditions for the HDS and HDN reactions were 3.0 MPa, 603 and 623 K, WHSV = 6 h^{-1} and H_2/oil = 500 (v/v). Liquid products were collected every hour after a stabilization period of 6 h. Both feed and products were analyzed using a FULI 9790 gas chromatograph equipped with an FID detector and an OV-101 column. The DBT and quinoline conversions and turnover frequency (TOF) [11] were used to evaluate the catalyst activity.

3. Results and discussion

3.1. Synthesis of bulk and supported ruthenium phosphide

As shown in Fig. 2, the typical diffraction peaks of Ru_2P are clearly shown. All peaks of the sample are close to the values reported in the Joint Committee on Powder Diffraction Standards (JCPDS) card no. 65-2382, which indicates the formation of bulk Ru_2P. In order to observe the peaks of products clearly, 10 wt% supported ruthenium phosphides were synthesized. Fig. 3 gave the XRD patterns of the samples prepared from the supported precursors (MCM-41) at 673 K, which consist of NaH_2PO_2 and $RuCl_3$•$3H_2O$ with different molar ratios ($NaH_2PO_2/RuCl_3$). The results show that Ru/MCM-41, Ru_2P/MCM-41, and RuP/MCM-41 could be synthesized at the molar ratio of 1.75, 3.5, and 5.75,

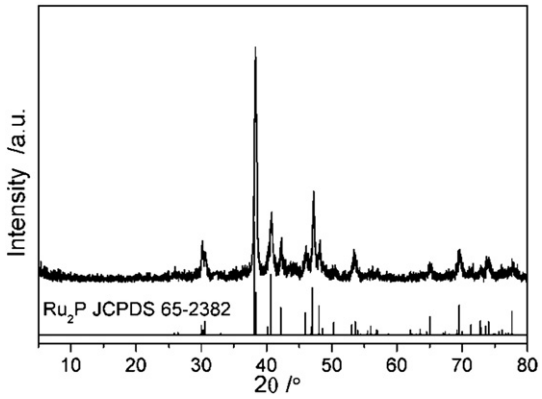

Fig. 2. The XRD pattern of the bulk Ru_2P prepared from the precursors, which consist of NaH_2PO_2•H_2O and $RuCl_3$•$3H_2O$ in a molar ratio of 3.5.

respectively. The diffraction peaks of Ru and Ru_2P, Ru_2P and RuP were detected when the molar ratio is 2.0, 5.0 , respectively.

Fig. 4 gave the XRD patterns of the samples prepared from the supported precursors (MCM-41), which consist of NaH_2PO_2•H_2O and $RuCl_3$•$3H_2O$ in a molar ratio of 3.5 at different calcination temperatures for 1 h. We can see that only diffraction peaks of Ru_2P were found when the precursor was heated to 673 K. Similarly, the diffraction peaks of Ru_2P were significantly enhanced when the

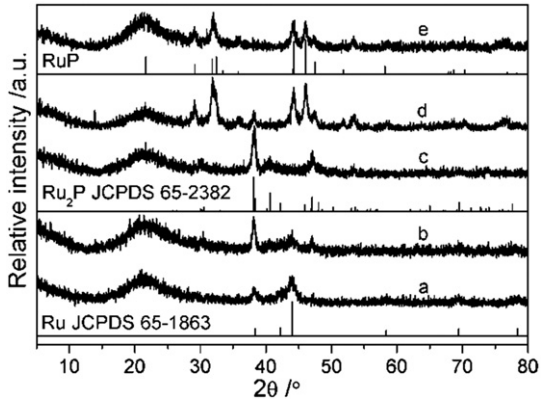

Fig. 3. The XRD patterns of the samples prepared from the supported precursors (MCM-41) at 673 K, which consist of NaH_2PO_2 and $RuCl_3$•$3H_2O$ with different molar ratios ($NaH_2PO_2/RuCl_3$): (a) 1.75, (b) 2.00, (c) 3.50, (d) 5.0, (e) 5.75.

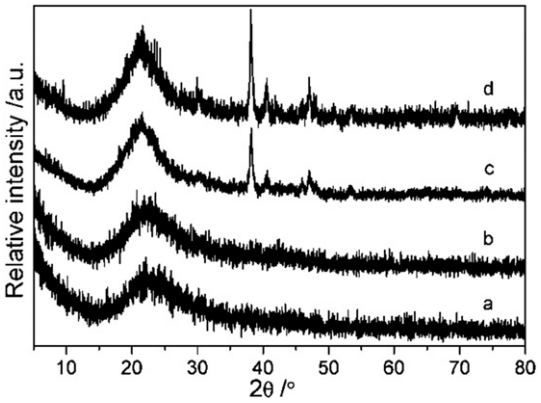

Fig. 4. The XRD patterns of the samples prepared from the supported precursors (MCM-41), which consist of $NaH_2PO_2 \cdot H_2O$ and $RuCl_3 \cdot 3H_2O$ in a molar ratio of 3.5 at different calcination temperatures for 1 h: (a) 573 K, (b) 623 K, (c) 673 K, (d) 773 K.

calcination temperature increased to 773 K, which indicates a sinter of Ru_2P. Hence, for supported catalysts, 673 K is a more appropriate temperature. In this paper, the loading of the catalysts used in HDS and HDN is 5 wt%. The TEM image of the as-prepared 5 wt% Ru_2P/MCM-41 was given in Fig. 5, which shows the average particle size of Ru_2P nanoparticles is about 10 nm. A magnified high resolution TEM image of the selected frame from Fig. 5a given in Fig. 5b, yields d-spacing values of 0.234 and 0.448 nm, respectively, for the (2 1 0) and (1 0 1) crystallographic planes of Ru_2P, which are in good agreement with the calculated values (JCPDS 65-2382). It indicates the formation of nanocrystalline Ru_2P on the MCM-41 support. Furthermore, the impact of different heating rates on the products was also studied (Supplementary material, Fig. S1). The XRD patterns show that Ru_2P is not affected by the heating rate. Table S1 and Fig. S2 (Supplementary material) display the textural properties of different samples. As expected, the supported catalysts reveal a lower S_{BET} specific areas and pore volumes with respect to pure support.

3.2. Catalytic activity

The DBT and quinoline conversions and turnover frequency (TOF) were used to evaluate the HDS and HDN activity [17,18]. The TOF was calculated using Eq. 1 (Supplementary material). Irreversible CO uptake measurements were used to titrate the surface metal atoms and to provide an estimate of the active sites on the catalysts [19]. Table 1 and Table S2 show the CO uptakes and catalytic activity of different catalysts. The low CO uptakes of the as-prepared catalysts indicated that there might be some of sinterring. The activity results show that Ru_2P/MCM-41 and RuP/MCM-41 catalysts both exhibited the higher activities than Ru/MCM-41, which is similar to those reported in the literature [10]. The products of DBT hydrodesulfurization are mainly about biphenyl (BP), cyclohexylbenzene (CHB), and bicyclohexane (BCH). The product selectivities of the Ru_2P/MCM-41 and RuP/MCM-41catalysts indicate that the hydrogenation (HYD) pathway is favored for DBT HDS over ruthenium phosphide catalysts. The catalytic activities of Ru_2P/MCM-41 and RuP/MCM-41 catalysts were lower than that of commercial NiMoWS catalyst, which may be due to lack of optimization of the catalysts. However, the supported ruthenium phosphide catalysts need in-depth study.

3.3. Investigation of the formation process

In our previous research [11], the formation of Ni_2P occurs by direct reduction of $NiCl_2$ with PH_3 produced by thermal decomposition of NaH_2PO_2. However, compared with nickel ions, ruthenium ions are reduced more easily. As shown in Fig. S3, the H_2-TPR patterns of different metal oxides indicated that RuO is reduced more easily than NiO. So the reaction mechanism of ruthenium phosphide may be different from nickel phosphide. We propose that several possible reactions occur.

$$2NaH_2PO_2 = PH_3\uparrow + Na_2HPO_4 \quad (1)$$

$$8RuCl_3 + 3PH_3 = 8Ru + 9HCl + 3PCl_5 \quad (2)$$

$$(1) \times 3 + (2) = (3)$$

$$8RuCl_3 + 6NaH_2PO_2 = 8Ru + 9HCl + 3PCl_5 + 3Na_2HPO_4 \quad (3)$$

$$4Ru + 2PH_3 = 2Ru_2P + 3H_2\uparrow \quad (4)$$

$$(3) + (4) \times 2 + (1) \times 4 = (5)$$

$$8RuCl_3 + 14NaH_2PO_2 = 4Ru_2P + 9HCl + 3PCl_5 + 7Na_2HPO_4 + 6H_2\uparrow \quad (5)$$

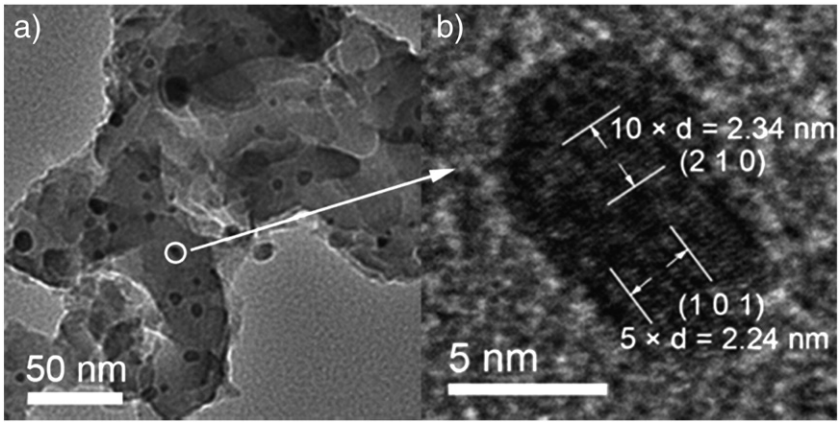

Fig. 5. The as-prepared Ru_2P/MCM-41 catalysts with loading of 5 wt% treated at 673 K for 1 h in an Ar atmosphere: (a) TEM micrograph, (b) the magnified HRTEM image of the selected frame from image (a).

Table 1
Conversion and product selectivity of DBT HDS on 5 wt% catalysts.

Catalysts	Conversion of DBT (%)			CO uptake ($\mu mol\ g^{-1}$)	TOF 603 K ($10^{-3}\ s^{-1}$)	Selectivity 623 K (%)		
	583 K	603 K	623 K			BP	BCH	CHB
Ru_2P/MCM-41	93.1	95.7	100	3.1	8.4	26.2	37.4	36.4
RuP/MCM-41	90.4	93.7	98.9	3.1	8.2	27.3	36.9	35.8
Ru/MCM-41	46.6	50.2	54.6	3.3	4.1	26.5	33.8	39.7
NiMoWS (commercial)	99.2	100	100	–	–	28.1	35.9	36.0

$$4Ru_2P + 2PH_3 = 4RuP + 3H_2\uparrow \quad (6)$$

$$(5) + (1) \times 4 + (6) \times 2 = (7)$$

$$8RuCl_3 + 22NaH_2PO_2 = 9HCl + 3PCl_5 + 11Na_2HPO_4 + 8RuP + 12H_2\uparrow \quad (7)$$

According to our previous research [11,12], NaH_2PO_2 could decompose and produce PH_3 when the temperature exceeds 473 K. According to Reaction (2), Ru was obtained when PH_3 was deficient, which was proved by the XRD patterns in Fig. 3a and b. We designed an experiment to prove that Ru_2P can be produced from Reaction (4), which consists of Ru/MCM-41 and NaH_2PO_2 as precursors and treated at 673 K for 1 h in static Ar. The diffraction peaks of Ru_2P were detected in the product, which indicates that Reaction (2) is existing (Supplementary material, Fig. S4). Reaction (5) shows that Ru_2P could be obtained by treating the precursor with NaH_2PO_2 and $RuCl_3$ in a molar ratio of 1.75 at 673 K. However, in our experiments, Ru_2P could not be obtained completely at this molar ratio, because there is a dead space in the reactor that is outside the temperature range and the bottom of the reactor was open. When the molar ratio is 1.75, pure metallic ruthenium was obtained, and this indicates that Ru^{3+} was reduced to Ru, but Ru_2P/MCM-41 could not be obtained at this molar ratio. When the molar ratio reached 2.0, a mixture of Ru and Ru_2P was obtained. Ru_2P/MCM-41 could be obtained at the molar ratio of 3.5. When the PH_3 is sufficient, it could be dissociated into hydrogen atoms and phosphorus atoms by Ru and Ru_2P at 673 K. At the same time, phosphorus atoms will further react with Ru and Ru_2P to form Ru_2P and RuP, which was similar to the formation of nickel phosphide [20]. The XRD result in Fig. 3d proved that Reaction (6) could occur at 673 K.

4. Conclusion

In summary, highly active Ru_2P/MCM-41 and RuP/MCM-41 catalysts were synthesized by thermal decomposition of ruthenium chloride and hypophosphite precursors. The catalytic activity results show that both Ru_2P/MCM-41 and RuP/MCM-41 catalysts exhibited higher activities than Ru/MCM-41. The results of investigation show that the reaction mechanism of ruthenium phosphide is different from nickel phosphide. Further studies will focus on the optimization of the supported Ru_2P and RuP catalysts.

Acknowledgements

The authors acknowledge financial support from the National Natural Science Foundation of China (grant no. 21073098), the Natural Science Foundation of Tianjin (11JCZDJC21600), and the Research Fund for MOE (IRT-0927), the Doctoral Program of Higher Education (20090031110015), and the Program for New Century Excellent Talents in University (NCET-10-0481).

Appendix A. Supplementary data

Supplementary data to this article can be found online at doi:10.1016/j.catcom.2011.08.005.

References

[1] S. Yang, C. Liang, R. Prins, J. Catal. 241 (2006) 465.
[2] E.L. Muetterties, J.C. Sauer, J. Am. Chem. Soc. 96 (1974) 3410.
[3] S.L. Brock, S.C. Perera, K.L. Stamm, Chem. Eur. J. 10 (2004) 3364.
[4] K.A. Gregg, S.C. Perera, G. Lawes, S. Shinozaki, S.L. Brock, Chem. Mater. 18 (2006) 879.
[5] J. Gopalakrishnan, S. Pandey, K.K. Rangan, Chem. Mater. 9 (1997) 2113.
[6] A.W. Burns, A.F. Gaudette, M.E. Bussell, J. Catal. 260 (2008) 262.
[7] H. Song, H. Yu, X. Wu, Y. Guo, J. Catal. 31 (2010) 447.
[8] S.F. Zaman, K.J. Smith, Appl. Catal. A 378 (2010) 59.
[9] A. Celzard, J.F. Marêché, G. Furdin, V. Fierro, C. Sayag, J. Pielaszek, Green Chem. 7 (2005) 784.
[10] Y. Kanda, C. Temma, K. Nakata, T. Kobayashi, M. Sugioka, Y. Uemichi, Appl. Catal. A-GEN. 386 (2010) 171.
[11] Q. Guan, W. Li, M. Zhang, K. Tao, J. Catal. 263 (2009) 1.
[12] Q. Guan, W. Li, J. Catal. 271 (2010) 413.
[13] A.V. Morozkin, Y.D. Seropegin, J. Alloys Compd. 365 (2004) 168.
[14] S. Rundqvist, Acta Chem. Scand. 14 (1960) 1961.
[15] S. Rundqvist, Acta Chem. Scand. 16 (1962) 287.
[16] C.M. Lukehart, S.B. Milne, Chem. Mater. 10 (1998) 903.
[17] Y.-K. Lee, S.T. Oyama, J. Catal. 239 (2006) 376.
[18] D. Nair, J.T. Scarpello, I. Vankelecom, L.M. Freitas Dos Santos, L.S. White, R.J. Kloetzing, T. Weltone, A.G. Livingston, Green Chem. 4 (2002) 319.
[19] S.T. Oyama, X. Wang, Y.-K. Lee, W.-J. Chun, J. Catal. 221 (2004) 263.
[20] S. Yang, C. Liang, R. Prins, J. Catal. 237 (2006) 118.